

Bilayer splitting in overdoped high T_c cuprates.

S. E. Barnes and S. Maekawa

Institute for Materials Research, Tohoku University, Sendai 980-8577, Japan

(Dated: November 13, 2018)

Recent angle-resolved photoemission data for overdoped Bi2212 are explained. Of the peak-dip-hump structure, the peak corresponds the $\vec{q} = 0$ component of a hole condensate which appears at T_c . The fluctuating part of this same condensate produces the hump. The bilayer splitting is large enough to produce a bonding hole and an electron antibonding quasiparticle Fermi surface. Smaller bilayer splittings observed in some experiments reflect the interaction of the peak structure with quasiparticle states near, but not at, the Fermi surface.

PACS numbers: 71.18.+y, 74.72.Hs, 79.60.Bm

The existence of a bilayer splitting remains a controversial issue. There are now two separate claims¹ to have observed via angle-resolved photoemission spectroscopy (ARPES) such a splitting in modest to heavily overdoped Bi2212 while others² have concluded that only a very small such splitting is possible for optimal or underdoped samples of the same material. The question of a possible bilayer splitting cannot be separated from the recent debate about the nature of the Fermi surface. Until recently the widely accepted Fermi surface was hole like³, however there have been several reports⁴ that, for different ARPES photon energies, an electronlike Fermi surface is seen. Very recently for a slightly overdoped Bi2212 it has been claimed⁵ that *both* electron *and* hole Fermi surfaces exist and that this reflects a modestly large bilayer splitting. These most recent experiments would seem to be in conflict with the earlier observation of a bilayer splitting. In the experiments¹ of Feng *et al.*, on a heavily overdoped sample the antibonding band was observed to cross the Fermi surface near $[\pi, 0]$ while the existence of an electronlike antibonding Fermi surface for a smaller hole doping is at odds with this observation.

In the picture developed here, as proposed⁵ by Bogdanov *et al.*, there exists a bilayer splitting which is sufficiently large that the bonding band is hole, while the antibonding band is electronlike. That part of the hole like antibonding band seen¹ by Feng *et al.*, which closes near $[\pi, 0]$, reflects, in fact, a near Fermi surface “shadow” resonance associated with an antibonding band which itself never crosses the Fermi surface.

For a bilayer the usual $t - J$ model becomes,

$$\mathcal{H} = - \sum_{ij\sigma\alpha\alpha'} t_{i\alpha j\alpha'} [\hat{c}_{i\sigma\alpha}^\dagger \hat{c}_{j\sigma\alpha'} + \text{H.c.}] + \sum_{ij\alpha\alpha'} J_{i\alpha j\alpha'} \vec{S}_{i\alpha} \cdot \vec{S}_{j\alpha}$$

where $\hat{c}_{i\sigma\alpha}^\dagger = (1 - n_{i-\sigma\alpha})c_{i\sigma\alpha}^\dagger$; $n_{i\sigma\alpha} = c_{i\sigma\alpha}^\dagger c_{i\sigma\alpha}$ and where $c_{i\sigma\alpha}^\dagger$ is for an electron of spin σ site i and plane α . The in-plane interactions are t and J and near-neighbor. The interplane exchange J_\perp is vertical, while the t_\perp leads to a single-particle bilayer splitting $(t_\perp/4)(\cos k_x - \cos k_y)^2$.

The present formalism signals a departure from the usual slave-boson method^{6,7}. Used here is a formalism based upon the Jordan-Wigner (JW) transformation⁸. The system is mapped to a one dimensional path. A

single spin fermion, f_i^\dagger creates an up spin at *path* site i when it acts on the down spin ferromagnetic vacuum $|\rangle_{-N/2}$. Here the total spin $S_z = -N/2$ and N is the (even) number of sites. A hole is created by b_i^\dagger . A hardcore constraint $Q_i = f_i^\dagger f_i + b_i^\dagger b_i \leq 1$ is needed *only for finite hole doping x*. *Fictitious unit flux tubes* perform the JW transformation. The tubes are reflected by *unitary* operators $u_i^\dagger = \exp[-i \int_0^{i-1} \vec{a} \cdot d\vec{r}]$ where \vec{a} is a vector potential for tubes attached to each particle.⁸ The raising operator $S_i^+ = f_i^\dagger u_i$ and destroys (in the sense $u_i u_i^\dagger = 1$) a flux tube before creating a spin particle, $S_{iz} = f_i^\dagger f_i - \frac{1}{2}(1 - b_i^\dagger b_i)$. The physical electron $\hat{c}_{i\uparrow}^\dagger = f_i^\dagger b_i$ while $\hat{c}_{i\downarrow}^\dagger = u_i^\dagger b_i$ involves a flux tube.

The standard mean-field slave-boson method introduces unphysical states because a certain constraint is obeyed only on average. The present development corrects this defect. This has important physical consequences. Within the usual approach, for doping x , the effective spin hopping matrix element $\sim (J + 2xt)/2 \sim 150$ meV which is sufficiently large to explain the strongly dispersive “quasiparticle” features indicated by solid circles in the ARPES data and theory of Fig. 1. In fact, this matrix element should be $J_e/2 = (J - 2xt)/2\sqrt{2}$ where the minus sign reflects the well-established fact that a small doping x favors ferromagnetism. Near optimal doping J_e is approximately zero. This J_e is involved principally in the dispersion of the so called “coherence peak,” i.e., the “+” and “|” in Fig. 1. The “quasiparticle” feature reflects a fluctuation part of the hole spectrum which is “driven” by the constraint. The physics of the b -particle hole Bose condensation is also changed when the constraint is enforced. Such a condensation needs the lowest energy level to be renormalized to the chemical potential and this results in a *gap equation* which determines T_c in both the underdoped *and* overdoped regimes. This paper introduces this interpretation of the ARPES data. In the process some rather subtle effects associated with the bilayer splitting are explained.

In analogy with the quantum Hall effect, the flux tubes reflected by the u_i^\dagger are nontrivial. That $\hat{c}_{i\uparrow}^\dagger = b_i^\dagger f_i$ while $\hat{c}_{i\downarrow}^\dagger = b_i^\dagger u_i$ suggests that $f_{i\alpha}$ and $u_{i\alpha}$ are intimately related. Important is the degeneracy of the vacuum. This

is $| - N/2 \rangle$, however, since \mathcal{H} is rotationally invariant, the ferromagnetic state $| - N/2 + 1 \rangle$ obtained by action of the *total spin* S^+ on $| - N/2 \rangle$ is equivalent. *Arbitrary* $N/2$ - f -particle states are of the form $\psi_{N/2} | - N/2 \rangle$ or $\phi_{N/2-1} | - N/2 + 1 \rangle$ where $\psi_{N/2}$ and $\phi_{N/2-1}$ are suitable field operators which create respectively $N/2$ and $N/2-1$, f particles. Consider $\hat{c}_{i\downarrow} = b_i^\dagger u_i$, it can be shown rigorously for large N and $M \sim N/2$, f particles,

$$\begin{aligned} & \langle -N/2 + 1 | \phi_{M-1}^\dagger b_i^\dagger u_i \psi_M | -N/2 \rangle \\ & = \langle -N/2 | \phi_{M-1}^\dagger b_i^\dagger f_i \psi_M | -N/2 \rangle. \end{aligned}$$

Thus the *vacuum off-diagonal matrix elements* involving u_i are equal to *vacuum diagonal* matrix elements with this operator replaced by f_i . Here u_i destroys a particle, as does f_i , but the destroyed particle appears in the vacuum so S_z is unchanged. A judicious choice of intermediate states is called for. With diagonal elements u_i is simply a phase factor, its particle nature only being manifest when the intermediate states introduce off-diagonal elements.

Corresponding to a "flux state", in the absence of doping and treating the flux at the mean-field level, the spectrum of the f particles is, $\mathcal{E}_{\vec{k}} = \sqrt{J_e^2 \gamma_{\vec{k}}^2 + \Delta_0^2 d_{\vec{k}}^2}$, where $\gamma_{\vec{k}} = (\cos k_x + \cos k_y)$ while $d_{\vec{k}} = (\cos k_x - \cos k_y)$. A $T = 0$, a relationship $J_e = \Delta_0 = J/\sqrt{2}$ reflects the unitary nature of the u_i .

Bose condensation involves the construction of a hole coherent state which satisfy the constraint. This is done by performing a $SO(3)$ rotation. The space for a given site i is spanned by the basis vectors $|\uparrow\rangle$, $|\downarrow\rangle$ and $|0\rangle$. The small rotation causes $|\sigma\rangle \rightarrow |\sigma\rangle + \theta_{\sigma i} |0\rangle$ while $|0\rangle \rightarrow |0\rangle - \sum_{\sigma} \theta_{\sigma i} |\sigma\rangle$. The rotation angle θ_i constitutes the wave function for the condensed holes. It is necessary to minimize the expectation value of \mathcal{H} with respect to this rotation. The result $(\partial\mathcal{H}/\partial\theta_i) = 0$ is of the form of an equation of motion for b_i^\dagger in which the energy has been equated to the chemical potential μ ; i.e., it amounts to the evident requirement that the lowest Bose level be renormalized to μ . The hopping term for these bosons is $-\sum t_{ij} u_i^\dagger b_i^\dagger b_j^\dagger u_j$, and the resulting diagonal term in \mathcal{H} is maximized in the negative sense when when $u_i \theta_{\downarrow i} = \theta$ a constant, while $u_i \theta_{\uparrow i} = \pm\theta$ where the sign alternates. Substituting this into $-\sum t_{ij} f_i^\dagger b_i^\dagger b_j^\dagger f_j$ and making the same mean-field approximation as used for the J term results in $-\theta^2(1/\sqrt{2}) \sum t_{ij} f_i^\dagger f_j$ which is without doubt ferromagnetic in nature, and $J_e = (J - 2xt)/\sqrt{2}$. A simple spin pair amplitude, e.g., $\langle f_{\vec{k}}^\dagger f_{-\vec{k}}^\dagger \rangle$, is forbidden by the constraint, however for half filling it is well known that the RVB state is reflected by a flux state amplitude $\langle f_{\vec{k}}^\dagger f_{\vec{k}+\vec{\pi}}^\dagger \rangle$, where $\vec{\pi} = (\pi, \pi)$. Since here the holes are subsumed into the spin particles, this result is extended to finite doping, i.e., with the above for $\theta_{\sigma i}$, it follows that the BCS pair amplitude $\langle \hat{c}_{\vec{k}\uparrow}^\dagger \hat{c}_{-\vec{k}\downarrow}^\dagger \rangle \approx \theta^2 \langle f_{\vec{k}}^\dagger f_{\vec{k}+\vec{\pi}}^\dagger \rangle$, i.e., the flux state plus *coherent* doping equals superconductivity.

The $O(3)$ rotation of \mathcal{H} introduces *new* θ^2 terms of physical importance. Since $|00\rangle$, reflecting near-neighbor hole sites, mixes with $|\downarrow 0\rangle$, while $|\downarrow\downarrow\rangle$ mixes with $|0\downarrow\rangle$, there is a b -particle pair term $-\theta^2 u_i^\dagger u_j b_i^\dagger b_j^\dagger + \text{H.c.}$ which results in a *charge gap* $K_c \sim 4\theta^2 t$. Rotating the physical electron operator $c_{i\sigma}^\dagger$ produces both $\theta_i f_{i\sigma}^\dagger$ and $\theta_i u_i^\dagger f_i^\dagger f_i$. The former *coherent* term implies that the condensate fraction is $c = \theta^2/2$ while the latter is corresponds to an *equal number* of constraint-driven *incoherent* fluctuating holes, this at zero temperature.

In other than one dimension, the Bose levels are renormalized towards μ by the $-\sum t_{ij} f_i^\dagger b_i^\dagger b_j^\dagger f_j$ term. Using the usual renormalization group techniques this results in a *gap equation*. High-energy intermediate states are integrated out down to some cutoff $K(\mu)$. Since the intermediate states involve both spin and charge degrees of freedom there are two contributions to $K(\mu) = K_s + K_c$. The charge pseudogap $K_c \sim 4\theta^2 t$ while $K_s \sim \mathcal{E}_{\vec{k}=\pi, \pi/2}$ reflects the width of the spin band due to both dispersion and the spin BSC gap. The $T = 0$ charge gap K_c is the lowest-energy scale and $T_c \sim K_c$, i.e., $T_c \propto c$. Spin pairing occurs at a higher mean-field temperature $T_s \sim J/2\sqrt{2}$ associated with the opening of a pseudogap. The scenario is supported the fact that $T_c \propto c$ and evidence⁹ of a pseudogap well above T_c , in tunneling for *overdoped* $\text{Bi}_2\text{Sr}_2\text{CuO}_{6+\delta}$ and via Zeeman splitting¹⁰ in $\text{Bi}_2\text{Sr}_2\text{CaCuO}_{8+\delta}$. With decreasing μ , when condensation first occurs, $K(\mu) = K_s$ ($K_c = 0$). This point is *unstable* precisely because $J_e = (J - 2xt)/\sqrt{2}$, whence K_s decreases with *increasing* x . In the underdoped region, when $\partial K_s/\partial x < 0$, the system separates into hole-rich regions with $(J - 2xt) \sim 0$ and with hole-poor regions between. Doping occurs at constant μ . In the overdoped region $\partial K_s/\partial x > 0$ and implies that K_c must decrease and with it the condensed fraction c and T_c . Up to this point the holes have been accommodated within the rotated f particles. Now b particles must be added and this requires that μ decreases. This must increase $K(\mu)$ which *slows* the flow out of the condensate with increasing x . These b -particle holes are not particularly important for ARPES. They are hard-core bosons which must avoid the existing condensed bosons. This implies a curvature to their wave functions which pushes their energy to at least $\sim 4xt$, i.e., out of range of the dispersive features near the Fermi surface. Their presence *is* seen in $J_e = (J - 2xt)/\sqrt{2}$ since this is a mean-field result and all of the holes must be counted in the x .

The physical electron Green's function $\mathcal{G}_{\vec{k}}$ describes the excitations of interest. Consider first a single plane. The operator—e.g., $\hat{c}_{i\uparrow}^\dagger \approx |b_i| f_i^\dagger + f_i^\dagger b_i^\dagger$ —contains a *condensate* part proportional to $|b_i| = \theta/\sqrt{2}$ and a *noncondensate* part reflected by b_i^\dagger . If within the Fourier transform of $-t \sum \hat{c}_{i\sigma}^\dagger \hat{c}_{j\sigma} = -2t \sum \gamma_{\vec{k}} \hat{c}_{\vec{k}\sigma}^\dagger \hat{c}_{\vec{k}\sigma}$ the *single* matrix element $\gamma_{\vec{k}}$ is removed, then all coherent motion of *holes* with this wave-vector is suppressed and this decouples these two parts of $\mathcal{G}_{\vec{k}}$. If $\mathcal{G}_{\vec{k}\ell}$ is the Green's function calculated

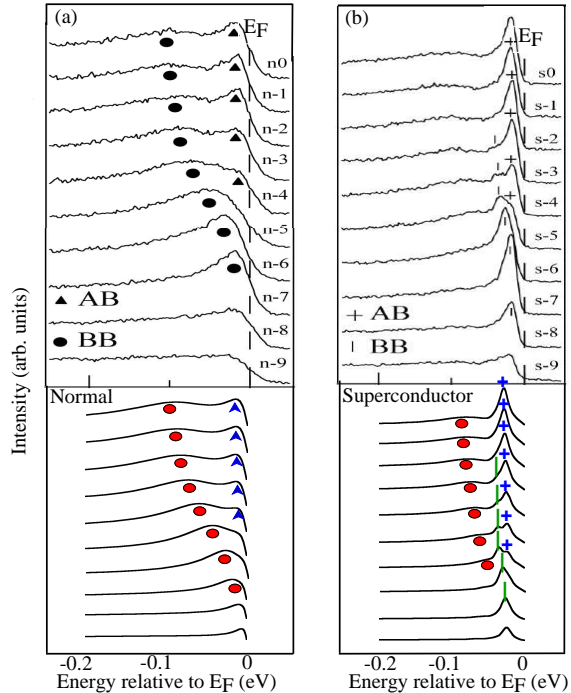


FIG. 1: (a) Experiment¹ (top) and theory (bottom) for the normal state. Theory corresponds to $\Im m \mathcal{G}_{a\vec{k}}$ with $s = 35$ meV, $\sqrt{ab} = 25$ meV $b = 0.65$, $d = 54$ meV and $e = 35$ meV for $k_y = \pi$ and $k_x = 0\pi, 0.025\pi, 0.05\pi, 0.075\pi \dots 0.225\pi$ in descending order. (b) The same for the superconducting state but with $s = 6$ meV, $\sqrt{ab} = 31$ meV $b = 1.15$, $d = 50$ meV and $e = 70$ meV. In both panels the strongly dispersive bonding band is indicated by a filled circle. For the normal state the triangles indicate the position of the weakly dispersive residue of the antibonding band while in the superconductive state the | and + indicate the positions of the coherence peaks associated with the bonding and antibonding bands, respectively. The rest of the parameters are given in the text.

without $\gamma_{\vec{k}}$, then trivially the full $\mathcal{G}_{\vec{k}}^{-1} = \mathcal{G}_{\vec{k}\ell}^{-1} - (-2t)\gamma_{\vec{k}}$. A simple case would ignore both pairing and the noncondensate part, whence $\mathcal{G}_{\vec{k}\ell}^{-1} = (\omega + is - J\gamma_{\vec{k}})/c$, leading to a $\mathcal{G}_{\vec{k}}^{-1}$ with poles at energy $\mathcal{E}_{\vec{k}} = (J - 2ct)\gamma_{\vec{k}}/\sqrt{2}$, with strength c , and illustrating the contribution of the condensate to J_e .

When the bilayer coupling is included, eigenstates are simultaneous eigenvectors of \mathcal{H} and a reflection operator R ; i.e., solutions, with index $a = \pm$, are bonding or antibonding respectively. Neutron data on the insulating compounds¹¹ suggest that the inter-plane J_{\perp} is vertical. The bonding and antibonding d -wave order parameters must then be *identical* for symmetry reasons and J_{\perp} is unimportant. With a bilayer splitting the condensate and noncondensate parts are decomposed by removing the matrix elements involving $\epsilon_{a\vec{k}} = -[2t\gamma_{\vec{k}} + a\frac{t_{\perp}}{4}(\cos k_x - \cos k_y)^2]$ (rather than $\gamma_{\vec{k}}$) and the Green's function becomes $\mathcal{G}_{a\vec{k}}(\omega + is) = [(G_{a\vec{k}s} + G_f)/(1 - \epsilon_{a\vec{k}} [G_{a\vec{k}s} + G_f])]$.

The full *condensate* contribution to $\mathcal{G}_{\vec{k}\ell}$ is easily seen

to be

$$G_{a\vec{k}} \equiv \frac{c}{\omega + is - ((x - c)\epsilon_{a\vec{k}} + J\gamma_{\vec{k}}) - \frac{|\Delta d_{\vec{k}}|^2}{\omega + is + (x\epsilon_{a-\vec{k}} + J\gamma_{-\vec{k}})}}, \quad (1)$$

where included are the complications associated with *both* pairing and the bilayer splitting via $\epsilon_{a\vec{k}}$. As described above, the important *noncondensate* part corresponds, in fact, to the fluctuations of the condensate driven by the constraint. At this stage in the development of the theory this is *modeled* by

$$G_f \equiv \frac{2(x_c - c)}{(\omega + is - \Sigma_f)}, \quad (2)$$

where $\Im m \Sigma_f = (a/\omega) + b(\omega - d)$ and where $\sqrt{ab} \sim K$. Then $\Re e \Sigma_f = e \operatorname{sgn}(\omega)$ and d also $\sim K$ result from shifts away from the Fermi surface due to the spin and charge gaps. In order to simulate finite temperatures, s is used to mimic thermal broadening, the condensed fraction c is treated as a parameter, and x_c is the total number of bosons including those in the fluctuating part of the condensate *but* excluding the b bosons mentioned above. The ARPES and tunneling are simulated using the resulting $\mathcal{G}_{a\vec{k}}(\omega + is)$.

Normal state ARPES spectra are calculated with the scale $K \sim 25$ meV with no holes condensed. With the other parameters $x \approx 0.2$, $J = 45$ meV, $2x_c t = 396$ meV and $2x_c t_{\perp} = 79$ meV, $\mathcal{G}_{a\vec{k}}(\omega + is)$ reproduces well the corresponding experimental spectrum of Feng et al.¹, Fig. 1a. The *bonding band* lies at a binding energy of $\sim 50 - 100$ meV and is quite broad. The peak which lies within ~ 20 meV of the Fermi surface for smaller k_x is a remnant of the *antibonding band* which lies *above* the Fermi surface. The strength of this antibonding band has been artificially increased by a factor of 2 in order to simulate the apparent experimental fact⁵ that under the conditions with which these spectra were taken, ARPES couples more strongly to the antibonding states. The nature of the near-Fermi-surface peaks for $\vec{k} = [\pi, 0]$ is not inconsistent with very recent data¹² for overdoped $\text{Bi}_2\text{Sr}_2\text{CaCu}_2\text{O}_8$. Experimentally the ratio of the normal-state peak and hump intensities can be varied via the photon energy which changes the relative coupling to the bonding and antibonding bands. Our simulations confirm *for this direction* that the hump and peak are predominantly of bonding and antibonding character, respectively.

The superconducting state implies hole condensation with a condensed fraction of 0.5, and with this coherence peaks develop near the Fermi surface. The thermal broadening reflected by $s = 6$ meV has been reduced. The reduction in the effect of thermal filling of the spin sector gap is reflected by an increased $K \sim 31$ meV. The other parameters are the same (see figure caption). A quasiparticle *bonding band*, again at a binding energy of $\sim 50 - 100$ meV, is identified in experiment spectra and indicated in the theory by a solid circle. The bonding

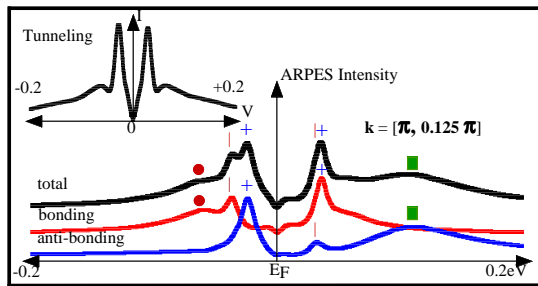


FIG. 2: The decomposition of theory into bonding and anti-bonding bands. The solid circle and square indicate the quasi-particle bands and the $|$ and $+$ the superconductive coherence peaks. The weight of the antibonding band is multiplied by 2 to simulate experiment. The inset shows theory for tunneling.

and antibonding coherence peaks identified by Feng *et al.*¹ are also indicated. The decomposition into bonding and antibonding bands for $\vec{k} = [\pi, 0.125\pi]$ is shown in Fig. 2. The antibonding band which lies above the Fermi surface “pulls” its coherence peak towards the Fermi surface, leading to an apparent gap of only ~ 20 meV. On the other hand, the full gap ~ 36 meV is exhibited by the coherence peak of the bonding band.

That the coherence peak splitting does *not* lead to a splitting of the tunneling spectrum, as it would in a simple BSC theory, is also illustrated by the inset in Fig. 2. This spectrum was obtained with identical parameters as for the body of this figure by averaging over 100 points in the Brillouin zone. It is interesting to note that the peak-dip-hump structure is reproduced with the dip at ~ 60 meV being consistent with typical tunneling data.¹³

The value of $J = 45$ meV reflects the gap via $\Delta =$

$J/\sqrt{2}$. This is small compared with $J = 120$ meV deduced from a fit to the spin waves.¹¹ However, a quantum correction¹¹ reduces the latter value to $J = 100$ meV. The same correction reduces the antiferromagnetic order parameter by $\sim 60\%$ and assuming a similar correction here increases the present J to ~ 74 meV. The difference is accounted for by a factor of $(1 - x)$ which arises for the $O(3)$ rotations and which was omitted in the above equations for clarity.

The value of $2x_c t_{\perp} = 79$ meV is larger than the value 45 meV deduced directly from experiment.¹ On the other hand, the larger bare value $t_{\perp} \approx 180$ meV agrees well with the local density approximation value.¹⁴ That there is a strong renormalization of t_{\perp} has been discussed elsewhere.¹⁵

While the present JW formalism is intended for all doping levels, the present application has been to the overdoped regime. As described above, the present approach suggests that the underdoped region phase separates into hole-rich and hole-poor regions where the concentration in the hole-rich regions corresponds approximately to optimal doping.¹⁶

This work was supported by a Grant-in-Ad for Scientific Research on Priority Areas from the Ministry of Education, Science, Culture and Technology of Japan, CREST. This work was mainly performed while SEB was on sabbatical leave from the Physics Department, University of Miami, FL, U.S.A. and he wishes to thank the members of IMR for their kind hospitality. The authors wish to thank D. L. Feng and Z. X. Shen for valuable communications about their work.

¹ D. L. Feng, N. P. Armitage, D. H. Lu, A. Damascelli, J. P. Hu, P. Bogdanov, A. Lanzara, F. Ronning, K. M. Shen, H. Eisaki, C. Kim, Z.-X. Shen, J. -I. Shimoyama, and K. Kishio, Phys. Rev. Lett. **86**, 5550 (2001); Y.-D. Chuang, A. D. Gromko, A. Fedorov, Y. Aiura, K. Oka, Y. Ando, H. Eisaki, S. I. Uchida, and D. S. Dessau, Phys. Rev. Lett. **87** 117002 (2001).

² J. Mesot, M. Randeria, M. R. Norman, A. Kaminski, H. M. Fretwell, J. C. Campuzano, H. Ding, T. Takeuchi, T. Sato, T. Yokoya, T. Takahashi, I. Chong, T. Terashima, M. Takano, T. Mochiku, and K. Kadowaki, Phys. Rev. B **63**, 224516 (2001).

³ P. Aebi, J. Osterwalder, P. Schwaller, L. Schlapbach, M. Shimoda, T. Mochiku, and K. Kadowaki, Phys. Rev. Lett. **72** 2757 (1994); Jian Ma, C. Quitmann, and R. J. Kelley, P. Alm eras, H. Berger, and G. Margaritondo, and M. Onellion, Phys. Rev. B **51** 3832 (1995); A. G. Loeser, Z.-X. Shen, D. S. Dessau, D. S. Marshall, C. H. Park, P. Fournier, and A. Kapitulnik, Science **273** 325 (1996); P. J. White, Z.-X. Shen, C. Kim, J. M. Harris, A. G. Loeser, P. Fournier, and A. Kapitulnik, Phys. Rev. B **54** 15669 (1996); H. Ding, A. F. Bellman, J. C. Campuzano, M. Randeria, M. R. Norman, T. Yokoya, T. Takahashi, H. Katayama-Yoshida, T. Mochiku, K. Kadowaki, G. Jennings, and G. P. Brivio,

Phys. Rev. Lett. **76** 1533 (1996); M. R. Norman, H. Ding, M. Randeria, J. C. Campuzano, T. Yokoya, T. Takeuchi, T. Takahashi, T. Mochiku, K. Kadowaki, P. Guptasarma, and D. G. Hinks, Nature **392** 157 (1998); N. L. Saini, J. Avila, A. Bianconi, A. Lanzara, M. C. Asensio, S. Tajima, G. D. Gu, and N. Koshizuka, Phys. Rev. Lett. **79** 3467 (1997).

⁴ Y.-D. Chuang, A. D. Gromko, D. S. Dessau, Y. Aiura, Y. Yamaguchi, K. Oka, A. J. Arko, J. Joyce, H. Eisaki, S. I. Uchida, S. I. Uchida, K. Nakamura, and Yoichi Ando, Phys. Rev. Lett. **83** 3717 (1999); D. L. Feng, W. J. Zheng, K. M. Shen, D. H. Lu, F. Ronning, J. Shimoyama, K. Kishio, G. Gu, D. V. der Marel, and Z.-X. Shen, cond-mat/9908056 (unpublished); A. D. Gromko, Y.-D. Chuang, D. S. Dessau, K. Nakamura, and Y. Ando, cond-mat/0003017 (unpublished).

⁵ P. V. Bogdanov, A. Lanzara, X. J. Zhou, S. A. Kellar, D. L. Feng, E. D. Lu, H. Eisaki, J.-I. Shimoyama, K. Kishio, Z. Hussain, and Z.-X. Shen Phys. Rev. B **64**, 180505 (2001).

⁶ S. E. Barnes, J. Phys. F **6** 115, 1375 (1976); J. Phys. F **7** 2637 (1976); Adv. Phys. **30** 801 (1980).

⁷ G. Baskaran, Z. Zuo and P. W. Anderson, Solid State Commun. **63**, 973 (1987).

⁸ S. E. Barnes and S. Maekawa, J. Phys. Condens. Matter

- 14**, L19, (2002); cond-mat/0111204 (unpublished).
- ⁹ M. Kugler, Ø. Fischer, C. Renner S. Ono and Y. Ando, Phys. Rev. Lett. **86**, 4911 (2001).
- ¹⁰ T. Shibauchi, L. Krusin-Elbaum, Ming Li, M. P. Maley, and P. H. Kes, Phys. Rev. Lett. **86**, 5763 (2001).
- ¹¹ D. Reznik, P. Bourges, H.F. Fong, L.P. Regnault, J. Bossy, C. Vettier, D.L. Milius, I.A. Aksay and B. Keimer, Phys. Rev. B **53** R14741 (1996).
- ¹² A. A. Kordyuk, S. V. Borisenko, T. K. Kim, K. Nenkov, M. Knupfer, M. S. Golden, J. Fink, H. Berger and R. Follath, Phys. Rev. Lett. **89** 077003 (1997).
- ¹³ see e.g., S. H. Pan, E. W. Hudson, A. K. Gupta, K.-W. Ng, H. Eisaki, S. Uchida, and J. C. Davis, Phys. Rev. Lett. **85**, 1536 (2000).
- ¹⁴ S. Chakravaty, A. Subdo, P.W. Anderson, S. Strong, Science **261**, 337 (1993); O. K. Anderson, A.I. Liechtenstein, O Jepsen, and F. Paulson, J. Phys. Chem Solids **12**, 1573 (1995).
- ¹⁵ A. I. Liechtenstein, O. Gunnarsson, O. K. Andersen, and R. M. Martin, Phys. Rev. B **54**, 12505 (1996); R. Eder, Y. Ohta, and S. Maekawa, Phys. Rev. B **51** 3265 (1995).
- ¹⁶ Experiment: C. Howald, P. Fournier and A. Kapitulnik, Phys. Rev. B **64** 100504 (2001); K. M. Lang, V. Madhavan, J.E. Hoffman, E.W. Hudson, H. Eisaki, S. Uchida, and J.C. Davis, Nature **415**, 412 (2002), manifests such a localization.